Impact-parameter dependence of the electromagnetic particle production in ultrarelativistic heavy-ion collisions

M. Vidović,[1,2] Martin Greiner,[3] C. Best,[1] and G. Soff[2]
[1] *Institut für Theoretische Physik, Johann Wolfgang Goethe-Universität, Postfach 111 932, D-6000 Frankfurt am Main, Germany*
[2] *Gesellschaft für Schwerionenforschung, Planckstrasse 1, Postfach 110 552, D-6100 Darmstadt, Germany*
[3] *Department of Physics, University of Arizona, Tucson, Arizona 85721*
(Received 24 August 1992)

The cross section for the electromagnetic production of different particles in heavy-ion collision is derived within the external field approach. Introducing polarized photon-fusion cross sections, it is possible to generalize the equivalent photon method to describe the impact-parameter dependence of the particle production. The impact-parameter dependent production of scalar and pseudoscalar (spin 0) bosons, charged (spin 0) boson pairs, and fermion pairs is discussed.

PACS number(s): 25.75.+r, 23.20.−g

I. INTRODUCTION

Ultrarelativistic heavy-ion collisions provide the opportunity to investigate particle production via the strong electromagnetic fields of heavy ions. A rough estimate of the collision time $t_{\rm coll} = R/\gamma$, where R denotes the nuclear radius and $\gamma = (1 - v^2/c^2)^{-1/2}$ is the Lorentz contraction factor, leads to a maximum frequency $\omega_{\rm max} \approx 1/t_{\rm coll} = \gamma/R$ contained in the electromagnetic field. For the proposed LHC (Large Hadron Collider) with $E_{\rm ion} = 3.5$ TeV/nucleon ($\gamma \simeq 3500$) and SSC (Superconducting Super Collider) with 8 TeV/nucleon ($\gamma \simeq 8000$) in a Pb+Pb collision this leads to $\omega_{\rm max} \approx 100$ GeV (LHC) and $\omega_{\rm max} \approx 250$ GeV (SSC). This mass regime exceeds the one which can be reached at existing e^+e^- colliders and is compatible with the one at $p\bar{p}$ colliders. As for an e^+e^- collider the electromagnetic production mechanism at a heavy-ion collider would be relatively clean, being in contrast to the situation at $p\bar{p}$ colliders, where the hadronic background is very large. Another advantage of heavy-ion collisions results from the Z^4 enhancement in the coherent production cross section over e^+e^- collisions, although the nuclear electromagnetic form factor suppresses this enhancement factor to some extent. On the other hand, the expected luminosities for a heavy-ion collider are considerably smaller than for an e^+e^- or $p\bar{p}$ collider.

For the theoretical description of the electromagnetic particle production in heavy-ion collisions the equivalent photon method [1–3] has been widely used because of its simplicity [4–17]. Within this method one replaces the electromagnetic fields of the moving heavy ion by an equivalent photon field, so that the production cross section in a heavy-ion collision can be approximated by the elementary two-photon fusion cross section folded with the equivalent photon distributions of both heavy ions. We are going to derive the equivalent photon method from first principles, i.e., directly from quantum electrodynamics (QED). This is one major subject of this paper. A subsequent publication [18] then is devoted to specific examples, which have not been considered up to now, such as the electromagnetic production and detectability of the Higgs boson of the minimal supersymmetric extension of the standard model, several mesons, glueballs, and supersymmetric particles.

Our paper is organized as follows. Using the external classical field approximation and applying the approximation, that the transverse momenta of the virtual photons are suppressed by the Lorentz factor γ with respect to their longitudinal momenta, we are able to derive the equivalent photon method from QED directly. As a byproduct of this derivation we also obtain an expression for the impact-parameter dependent equivalent photon production cross section. This expression is convenient to use to exclude the central collision region in the production cross section, which allows one to circumvent the large hadronic background in central collisions. It splits up into two contributions: For the scalar part the polarization vectors of the equivalent photons have to be parallel, whereas the polarization vectors have to be perpendicular for the pseudoscalar part. We also demonstrate that the scalar and pseudoscalar contributions, respectively, can be translated to the fact that the electromagnetic fields of the two colliding heavy ions have to be parallel or perpendicular, respectively. This is the subject of Sec. II. In Sec. III we discuss some immediate consequences and generalities for the impact-parameter dependent electromagnetic production of a scalar and pseudoscalar (spin 0) boson, a charged (spin 0) boson pair, and a fermion pair (spin 1/2). Conclusions will be presented in Sec. IV.

II. IMPACT-PARAMETER DEPENDENT EQUIVALENT PHOTON METHOD

A. The equivalent photon method

The electromagnetic field of a charged nucleus moving at high velocities becomes more and more transverse with respect to the direction of propagation. As a consequence, an observer in the laboratory frame cannot dis-

tinguish between the electromagnetic field of a relativistic nucleus and a bunch of equivalent photons; the electromagnetic field of a real photon is purely transverse.

For a relativistic heavy-ion collision this implies that the total cross section for electromagnetic processes like the electromagnetic creation of particles can be approximately described as a photon-photon fusion cross section folded with the equivalent photon distributions of the two nuclei:

$$\sigma^{WW}_{A_1A_2\to A_1A_2X} = \int\int d\omega_1\, d\omega_2\, n_{A_1}(\omega_1)\, n_{A_2}(\omega_2) \times \sigma_{\gamma\gamma\to X}(\omega_1,\omega_2) \quad . \tag{1}$$

The equivalent photon distribution can be derived explicitly by equating the energy flux (Poynting vector) of the transverse electromagnetic field of a nucleus through a transverse plane and the energy of the equivalent photon bunch; this yields [4]

$$n(\omega) = \frac{4Z^2\alpha}{\omega}\int \frac{\mathrm{d}^2k_\perp}{(2\pi)^2}\left(\frac{F(\mathbf{k}_\perp^2+\omega^2/\gamma^2)}{\mathbf{k}_\perp^2+\omega^2/\gamma^2}\right)^2 |\mathbf{k}_\perp|^2 \,, \tag{2}$$

where α is the fine structure constant, Z is the nuclear charge number, $\gamma = (1-v^2/c^2)^{-1/2}$ is the Lorentz contraction factor, and F is the nuclear charge form factor.

With the equivalent photon cross section (1) it is relatively easy to estimate the total production cross section for the electromagnetic creation of particles. This has been accomplished extensively in the past; for corresponding results we refer to the literature [4–17]. Instead we prefer to point out that the equivalent photon cross section (1) does not provide any information about the location of the particle production process. Tentatively one would expect that light particles are produced at large impact parameters whereas heavy particles should be generated at smaller impact parameters.

In particular, for very heavy particles, for example, Higgs bosons, supersymmetric, or technicolor particles, it is extremely important to know the impact-parameter dependence of the production cross section. From the experimental point of view electromagnetically produced particles should be discriminated from production mechanisms governed by strong interactions; therefore those small impact parameters, for which the two nuclei overlap and thus strongly interact, have to be excluded.

In order to derive the desired impact-parameter dependent cross section it suggests itself to start with Feynman diagrams directly. But at the end this might become quite involved numerically. On the other hand, it would be nice to save some of the simplicity of the equivalent photon approach. We will demonstrate that some straightforward and reasonable approximations to the S-matrix elements lead to a feasible expression for the impact-parameter dependent cross section, which upon integrating over the impact-parameter yields the equivalent photon cross section (1). This is an impact-parameter dependent generalization of the ordinary equivalent photon method. In this section, we first consider the general structure of the relevant S-matrix elements and the corresponding cross sections.

B. General structure of the S-matrix element and of the cross section

We will treat the electromagnetic field of the two nuclei classically: We assume both nuclei move with constant velocity on straight lines being separated by the impact parameter $\mathbf{b}$; small deflections from the straight lines due to the collision are neglected. Then the electromagnetic potentials in the Lorentz gauge $\partial_\nu A^\nu = 0$ follow from d'Alembert's equation, $\Box A^\mu = j^\mu$, where j^μ is the classical electromagnetic current of the moving nucleus. They read

$$A_1^\mu(k_1,b) = -2\pi Z_1 e\, e^{\mathrm{i}k_1^\tau b_\tau}\,\delta(k_1^\nu u_{1\nu})\,\frac{F(-k_1^\rho k_{1\rho})}{k_1^\sigma k_{1\sigma}}\,u_1^\mu \quad , \tag{3}$$

$$A_2^\mu(k_2,0) = -2\pi Z_2 e\,\delta(k_2^\rho u_{2\rho})\,\frac{F(-k_2^\rho k_{2\rho})}{k_2^\sigma k_{2\sigma}}\,u_2^\mu \quad .$$

The δ function assures the motion on a straight line with a constant velocity. The velocities of the two heavy ions, which from now on we will assume to be identical, $u_{1,2} = \gamma(1,0,0,\pm v)$, are taken in the collider system characterized by the Lorentz contraction factor γ (equal-speed system). $F(-k^2)$ denotes the nuclear charge form factor.

The amplitude for the creation of new particles via the electromagnetic fields of the two nuclei is given by the S-matrix element. In lowest order in the electromagnetic potentials A_1^μ, A_2^μ of the two nuclei it exhibits the following general structure [19] :

$$S(P\alpha,\mathbf{b}) = \int\frac{d^4k_1}{(2\pi)^4}\int\frac{d^4k_2}{(2\pi)^4}\,[A_1^\mu(k_1,\mathbf{b})\,\Gamma_{\mu\nu}(k_1k_2;P\alpha)\,A_2^\nu(k_2,0)\,](2\pi)^4\delta^4(k_1+k_2-P) \quad . \tag{4}$$

Here P means the total momentum of the produced particles, α their remaining phase-space coordinates, and $\mathbf{b}$ the impact parameter. $\Gamma_{\mu\nu}$ indicates the vertex function; its explicit structure depends on the nature of the created particles.

For example, for the production of a scalar boson the vertex function is given by

$$\Gamma_{\mu\nu}(k_1k_2;P\alpha) = g_\mathrm{s}\,[(k_1^\sigma k_{2\sigma})\,g_{\mu\nu} - k_{1\nu}k_{2\mu}] \quad , \tag{5}$$

and the vertex function for the production of a pseudoscalar boson reads

$$\Gamma_{\mu\nu}(k_1k_2;P\alpha) = g_\mathrm{ps}\epsilon_{\mu\nu\sigma\tau}k_1^\sigma k_2^\tau \quad . \tag{6}$$

For the production of a charged pair of bosons or fermions the lowest- (second-) order vertex function can be found in standard textbooks [19] and will not be given here.

The vertex function multiplied with the δ function can

be interpreted as a transition current,

$$J_{\mu\nu}(k_1k_2;P\alpha) = \Gamma_{\mu\nu}(k_1k_2;\alpha)\,(2\pi)^4\delta^4(k_1+k_2-P) \quad , \tag{7}$$

so that the S-matrix element (4) may be written as

$$S(P\alpha,\mathbf{b}) = \int \frac{d^4k_1}{(2\pi)^4} \int \frac{d^4k_2}{(2\pi)^4}\, A_1^\mu(k_1,\mathbf{b})\, A_2^\nu(k_2,0) \times J_{\mu\nu}(k_1k_2;P\alpha)\,. \tag{8}$$

The transition current is conserved, i.e.,

$$k_1^\mu J_{\mu\nu} = k_2^\nu J_{\mu\nu} = 0 \quad , \tag{9}$$

which follows quite generally from the gauge invariance of the S-matrix element.

For our following considerations the explicit expression for the transition current is irrelevant; it is only important that it acts like a conserved current (9) and contains a δ function (7) for the four-momentum conservation.

Performing the integrals over the δ functions, Eq. (8) becomes, with $Z_1 = Z_2 = Z$ and $F_1 = F_2 = F$,

$$S(P\alpha;\mathbf{b}) = Z^2\frac{e^2}{2\gamma^2}\int \frac{d^2k_\perp}{(2\pi)^2}\,\frac{F(-k_1^2)}{-k_1^2}\,\frac{F(-k_2^2)}{-k_2^2} \times u_{1\mu}u_{2\nu}\Gamma^{\mu\nu}(k_1k_2;\alpha)\,e^{-i\mathbf{b}\cdot\mathbf{k}_\perp}, \tag{10}$$

where the factor $1/(2\gamma^2)$ results from the integration over the δ functions appearing in the electromagnetic four-potential (3); the photon momenta are

$$k_1 = (\omega_1,\mathbf{k}_\perp,\omega_1/v)\,, \quad k_2 = (\omega_2,\mathbf{P}_\perp-\mathbf{k}_\perp,-\omega_2/v)\,, \tag{11}$$
$$\omega_1 = \tfrac{1}{2}(P_0+vP_z), \quad \omega_2 = \tfrac{1}{2}(P_0-vP_z).$$

Here the subscript $\perp$ indicates the perpendicular plane, i.e., the plane perpendicular to the motion of the nuclei.

Given the S-matrix element as in Eq. (10), the total cross section for the electromagnetic production of particles follows from the square of the S-matrix element integrated over the phase space of the n outgoing created particles $\tilde{d}p_1\cdots\tilde{d}p_n$ and integrated over the impact parameter. We introduce the total momentum P in the phase-space element explicitly:

$$\tilde{d}p_1\cdots\tilde{d}p_n = \frac{d^4P}{(2\pi)^4}\,\mathrm{d}\alpha \quad , \tag{12}$$

where $d\alpha$ means the phase-space element of the restricted phase space

$$d\alpha = d\alpha\,|_P = \tilde{d}p_1\cdots\tilde{d}p_n\,(2\pi)^4\,\delta^4(p_1+\cdots+p_n-P) \quad . \tag{13}$$

For the cross section we then obtain

$$\begin{aligned}\sigma &= \int d^2b \int |S(P\alpha;\mathbf{b})|^2 \frac{d^4P}{(2\pi)^4}\,d\alpha \\ &= \frac{Z^4e^4}{2\gamma^4}\int d^2b \int \frac{d\omega_1}{2\pi}\frac{d\omega_2}{2\pi}\frac{d^2k_{1\perp}}{(2\pi)^2}\frac{d^2k_{2\perp}}{(2\pi)^2}\frac{d^2q_\perp}{(2\pi)^2}\,\frac{F(-k_1^2)}{-k_1^2}\,\frac{F(-k_2^2)}{-k_2^2}\,\frac{F^*(-k_1'^2)}{-k_1'^2}\,\frac{F^*(-k_2'^2)}{-k_2'^2}\,e^{-i\mathbf{b}\cdot\mathbf{q}_\perp}\,u_{1\mu}u_{2\nu}u_{1\mu'}u_{2\nu'} \\ &\quad\times \int \Gamma^{\mu\nu}(k_1k_2;\alpha)\,\Gamma^{\mu'\nu'*}(k_1'k_2';\alpha)\,d\alpha\Big|_{P=(\omega_1+\omega_2,\mathbf{k}_{1\perp}+\mathbf{k}_{2\perp},(\omega_1-\omega_2)/v)}\,,\end{aligned} \tag{14}$$

where we integrate over the new variables

$$\mathbf{k}_{2\perp} = \mathbf{P}_\perp - \mathbf{k}_{1\perp}$$

and (15)

$$\mathbf{q}_\perp = \mathbf{k}_{1\perp} - \mathbf{k}'_{1\perp}$$

instead of $\mathbf{P}_\perp$ and $\mathbf{k}'_\perp = \mathbf{k}'_{1\perp}$. In the case of particles with spin the integration over the restricted phase-space element $d\alpha$ goes along with a summation over spin quantum numbers. The photon momenta now are

$$\begin{aligned} k_1 &= (\omega_1,\mathbf{k}_{1\perp},\omega_1/v)\,, \quad k_2 = (\omega_2,\mathbf{k}_{2\perp},-\omega_2/v)\,, \\ k_1' &= (\omega_1,\mathbf{k}_{1\perp}-\mathbf{q}_\perp,\omega_1/v)\,, \\ k_2' &= (\omega_2,\mathbf{k}_{2\perp}+\mathbf{q}_\perp,-\omega_2/v)\,. \end{aligned} \tag{16}$$

Before we turn our attention to the relevant approximations to be performed in order to derive from (14) the equivalent photon cross section (1), we first have to consider the general structure of the real photon-photon fusion cross section. It is this quantity which has to be extracted from expression (14).

C. The elementary photon-photon fusion cross section

The elementary photon-photon fusion cross section is governed by the invariant matrix element

$$\mathcal{M}(k_1k_2;P\alpha) = \epsilon_{1\mu}\epsilon_{2\nu}\Gamma^{\mu\nu}(\omega_1\omega_2;\alpha), \tag{17}$$

where $\Gamma^{\mu\nu}(\omega_1\omega_2;\alpha)$ again represents the vertex function as in the preceeding section. The two real photons are assumed to be collinear and have momenta $k_1 = (\omega_1,0,0,\omega_1)$, $k_2 = (\omega_2,0,0,-\omega_2)$. We choose their polarization vectors to be in the perpendicular plane: $\epsilon_\mu = (0,\boldsymbol{\epsilon}_\perp,0)$ with $\boldsymbol{\epsilon}_\perp^2 = 1$.

The polarized cross section is obtained by squaring the matrix element $\mathcal{M}(k_1k_2;P\alpha)$, integrating over the phase space of the created particles, and dividing through a flux factor:

$$\sigma(\omega_1,\omega_2,\epsilon_{1\perp},\epsilon_{2\perp}) = \frac{1}{8\omega_1\omega_2}\epsilon_{1i}\epsilon_{2j}\epsilon_{1i'}\epsilon_{2j'}\int \Gamma^{ij}(\omega_1\omega_2;\alpha)\Gamma^{i'j'*}(\omega_1\omega_2;\alpha)\,(2\pi)^4\delta^4(k_1+k_2-P)\,\frac{d^4P}{(2\pi)^4}\,d\alpha \tag{18}$$

(Latin indices run only over the perpendicular plane). After performing the integral over the total momentum, the total cross section for polarized photons reads

$$\begin{aligned}\sigma(\omega_1,\omega_2;\epsilon_{1\perp},\epsilon_{2\perp}) &= \frac{1}{8\omega_1\omega_2}\epsilon_{1i}\epsilon_{2j}\epsilon_{1i'}\epsilon_{2j'}\int \Gamma^{ij}(\omega_1\omega_2;\alpha)\Gamma^{i'j'*}(\omega_1\omega_2;\alpha)\,d\alpha\Big|_{P=(\omega_1+\omega_2,0,0,\omega_1-\omega_2)}\\ &\equiv \epsilon_{1i}\epsilon_{2j}\epsilon_{1i'}\epsilon_{2j'}\eta^{iji'j'}(\omega_1,\omega_2)\quad .\end{aligned} \tag{19}$$

The form of the tensor $\eta^{iji'j'}$ can be deduced from the study of its transformation behavior. Since the total polarized cross section is invariant under rotations in the perpendicular plane, we may choose one polarization vector to point along the x direction whereas the other one may be characterized by an angle φ: $\epsilon_{1\perp}=(1,0)$ and $\epsilon_{2\perp}=(\cos\varphi,\sin\varphi)$. Inserting this into (19) and requiring additional invariance under reflection $\varphi\to-\varphi$, one finds the following form for the cross section:

$$\begin{aligned}\sigma(\omega_1,\omega_2;\epsilon_{1\perp},\epsilon_{2\perp}) &= \cos^2\varphi\,\eta^{1111}(\omega_1,\omega_2)+\sin^2\varphi\,\eta^{1212}(\omega_1,\omega_2)\\ &= \cos^2\varphi\;\sigma_{\rm s}(\omega_1,\omega_2)+\sin^2\varphi\;\sigma_{\rm ps}(\omega_1,\omega_2)\\ &= (\epsilon_{1\perp}\cdot\epsilon_{2\perp})^2\,\sigma_{\rm s}(\omega_1,\omega_2)+(\epsilon_{1\perp}\times\epsilon_{2\perp})^2\,\sigma_{\rm ps}(\omega_1,\omega_2)\quad .\end{aligned} \tag{20}$$

The cross section consists of two parts $\sigma_{\rm s}$ and $\sigma_{\rm ps}$. The subscripts s and ps stand for scalar and pseudoscalar, respectively, because the polarizations of the two incoming photons are either parallel or perpendicular to each other. The average over the polarizations yields the total unpolarized cross section

$$\sigma(\omega_1,\omega_2) = \frac{\sigma_{\rm s}(\omega_1,\omega_2)+\sigma_{\rm ps}(\omega_1,\omega_2)}{2}\quad . \tag{21}$$

It is crucial to distinguish between the polarized scalar and pseudoscalar cross sections. As we will see later only the scalar cross section contributes to the scalar boson production, whereas only the pseudoscalar cross section contributes to the pseudoscalar boson production. On the other hand, the cross section for the production of a charged boson pair or a fermion pair is a mixture of the scalar and pseudoscalar part.

With the introduction of the two-dimensional matrices

$$\kappa_{\rm s}^{ij} = \begin{pmatrix}1 & 0\\ 0 & 1\end{pmatrix}$$

and (22)

$$\kappa_{\rm ps}^{ij} = \begin{pmatrix}0 & 1\\ -1 & 0\end{pmatrix}\quad ,$$

it is also possible to express the tensor $\eta^{iji'j'}$ with respect to $\sigma_{\rm s}$ and $\sigma_{\rm ps}$:

$$\eta^{iji'j'}(\omega_1,\omega_2) = \kappa_{\rm s}^{ij}\kappa_{\rm s}^{i'j'}\,\sigma_{\rm s}(\omega_1,\omega_2)+\kappa_{\rm ps}^{ij}\kappa_{\rm ps}^{i'j'}\,\sigma_{\rm ps}(\omega_1,\omega_2). \tag{23}$$

D. Equivalent photon approach to the impact-parameter dependent cross section

Now we introduce some reasonable approximations, which take into account the equivalent photon character of the virtual photons from the electromagnetic fields of the colliding nuclei, and connect the cross section (14) with the underlying two-photon cross section (19). Since we deal with the conserved transition current $J^{\mu\nu}$, cf. Eq. (9), its timelike coordinate may be expressed by its spacelike components:

$$\begin{aligned}J^{0\nu}(k_1k_2;P\alpha) &= -\frac{k_{1i}J^{i\nu}+k_{1z}J^{3\nu}}{k_{10}}\quad ,\\ J^{\mu0}(k_1k_2;P\alpha) &= -\frac{k_{2i}J^{\mu i}+k_{2z}J^{\mu3}}{k_{20}}.\end{aligned} \tag{24}$$

The nuclei move on straight trajectories and thus $k_z/k^0=\pm1/v$, confer Eq. (11). We obtain

$$\begin{aligned}u_{1\mu}u_{2\nu}J^{\mu\nu} = \gamma^2\frac{k_{1i}}{k_{10}}\frac{k_{2j}}{k_{20}}J^{ij}+\frac{1}{v}\left(\frac{k_{2j}}{k_{20}}J^{3j}-\frac{k_{1i}}{k_{10}}J^{i3}\right)\\ -\frac{1}{\gamma^2v^2}J^{33}\quad .\end{aligned} \tag{25}$$

Precisely at this point we introduce the decisive approximations, which will lead to the equivalent photon result. The term ω/γ, which corresponds to k_0/γ or k_3/γ, is of the same order of magnitude as the term $|\mathbf{k}_\perp|$, which corresponds to k_i:

$$|\mathbf{k}_\perp| \approx \frac{1}{\gamma}|\mathbf{k}_\parallel| \approx \frac{\omega}{\gamma}\quad . \tag{26}$$

This can be verified by considering those values of $|\mathbf{k}_\perp|$, which contribute most in the integrand of the equivalent photon distribution (2). The same relation also holds, if one compares the transverse component of the Poynting vector to its longitudinal one.

For the scalar boson the dominant contribution in Eq. (25) originates from the first term; the second and third terms are suppressed by a factor of $1/\gamma^2$ with respect to the first one. The situation for the pseudoscalar boson (6), the charged boson pair, and the fermion pair is exactly the same.

As a consequence of all these considerations, Eq. (25) can now safely be approximated by

$$u_{1\mu}u_{2\nu}J^{\mu\nu}(k_1k_2;P\alpha) \approx \gamma^2 \frac{k_{1i}}{\omega_1}\frac{k_{2j}}{\omega_2} J^{ij}(\omega_1\omega_2;P\alpha) \quad , \tag{27}$$

or written only in terms of the vertex function,

$$u_{1\mu}u_{2\nu}\Gamma^{\mu\nu}(k_1k_2;\alpha) \approx \gamma^2 \frac{k_{1i}}{\omega_1}\frac{k_{2j}}{\omega_2}\Gamma^{ij}(\omega_1\omega_2;\alpha). \tag{28}$$

On the right-hand side now appears the vertex function for real photons as in (19). This identification is the heart of the equivalent photon approach.

Introducing approximation (28) in the cross section (14) leads to

$$\begin{aligned}\sigma = \frac{Z^4e^4}{2}\int d^2b \int\frac{d\omega_1}{2\pi}\int\frac{d\omega_2}{2\pi}\int\frac{d^2k_{1\perp}}{(2\pi)^2}\int\frac{d^2k_{2\perp}}{(2\pi)^2}\int\frac{d^2q_\perp}{(2\pi)^2}\, e^{-i\mathbf{b}\cdot\mathbf{q}_\perp}\frac{k_{1i}}{\omega_1}\frac{k_{2j}}{\omega_2}\frac{k_{1i'}-q_{i'}}{\omega_1}\frac{k_{2j'}+q_{j'}}{\omega_2}\\ \times\mathcal{F}_1(\mathbf{k}_{1\perp},\omega_1)\,\mathcal{F}_2(\mathbf{k}_{2\perp},\omega_2)\,\mathcal{F}_1^*(\mathbf{k}_{1\perp}-\mathbf{q}_\perp,\omega_1)\,\mathcal{F}_2^*(\mathbf{k}_{2\perp}+\mathbf{q}_\perp,\omega_2)\\ \times\int\Gamma^{ij}(\omega_1\omega_2;\alpha)\Gamma^{i'j'*}(\omega_1\omega_2;\alpha)\,d\alpha\Big|_{P=(\omega_1+\omega_2,0,0,\omega_1-\omega_2)}\end{aligned} \tag{29}$$

with $\mathcal{F}(\mathbf{k}_\perp,\omega) = F(-k^2)/(-k^2)$. Using Eqs. (19) and (23) the last integral can be identified with the polarized real photon–photon fusion cross sections:

$$\int\Gamma^{ij}(\omega_1\omega_2;\alpha)\Gamma^{i'j'*}(\omega_1\omega_2;\alpha)\,d\alpha\Big|_{P=(\omega_1+\omega_2,0,0,\omega_1-\omega_2)} = 8\omega_1\omega_2\left[\kappa_{\rm s}^{ij}\kappa_{\rm s}^{i'j'}\,\sigma_{\rm s}(\omega_1,\omega_2)+\kappa_{\rm ps}^{ij}\kappa_{\rm ps}^{i'j'}\,\sigma_{\rm ps}(\omega_1,\omega_2)\right] \quad , \tag{30}$$

so that the cross section (29) can be cast in the following form:

$$\begin{aligned}\sigma = 16\frac{Z^4e^4}{(4\pi)^2}\int d^2b\int\frac{d\omega_1}{\omega_1}\int\frac{d\omega_2}{\omega_2}\int\frac{d^2k_{1\perp}}{(2\pi)^2}\int\frac{d^2k_{2\perp}}{(2\pi)^2}\int\frac{d^2q_\perp}{(2\pi)^2}\,e^{-i\mathbf{b}\cdot\mathbf{q}_\perp}\\ \times\mathcal{F}_1(\mathbf{k}_{1\perp},\omega_1)\,\mathcal{F}_2(\mathbf{k}_{2\perp},\omega_2)\,\mathcal{F}_1^*(\mathbf{k}_{1\perp}-\mathbf{q}_\perp,\omega_1)\,\mathcal{F}_2^*(\mathbf{k}_{2\perp}+\mathbf{q}_\perp,\omega_2)\\ \times\{(\mathbf{k}_{1\perp}\cdot\mathbf{k}_{2\perp})\,((\mathbf{k}_{1\perp}-\mathbf{q}_\perp)\cdot(\mathbf{k}_{2\perp}+\mathbf{q}_\perp))\,\sigma_{\rm s}(\omega_1,\omega_2)\\ +(\mathbf{k}_{1\perp}\times\mathbf{k}_{2\perp})\cdot((\mathbf{k}_{1\perp}-\mathbf{q}_\perp)\times(\mathbf{k}_{2\perp}+\mathbf{q}_\perp))\,\sigma_{\rm ps}(\omega_1,\omega_2)\}\end{aligned} \quad . \tag{31}$$

Now we prove that the total cross section (31) is indeed identical to the equivalent photon cross section (1). The integration over the impact parameter $\mathbf{b}$ leads to a δ function in the transverse momentum $\mathbf{q}_\perp$, i.e., $\delta(\mathbf{q}_\perp)$, so that it follows for (31):

$$\begin{aligned}\sigma &= 16\frac{Z^4e^4}{(4\pi)^2}\int\frac{d\omega_1}{\omega_1}\int\frac{d\omega_2}{\omega_2}\int\frac{d^2k_{1\perp}}{(2\pi)^2}\,|\mathcal{F}_1(\mathbf{k}_{1\perp},\omega_1)|^2\int\frac{d^2k_{2\perp}}{(2\pi)^2}\,|\mathcal{F}_2(\mathbf{k}_{2\perp},\omega_2)|^2\\ &\quad\times\left[(\mathbf{k}_{1\perp}\cdot\mathbf{k}_{2\perp})^2\,\sigma_{\rm s}(\omega_1,\omega_2)+|(\mathbf{k}_{1\perp}\times\mathbf{k}_{2\perp})|^2\,\sigma_{\rm ps}(\omega_1,\omega_2)\right]\\ &= \int d\omega_1\int d\omega_2\; n_1(\omega_1)\,n_2(\omega_2)\,\sigma(\omega_1,\omega_2) \quad ,\end{aligned} \tag{32}$$

where we have used Eqs. (2) and (21) in the last step. This is the equivalent photon cross section (1). One should keep in mind that the only applied approximation to the exact result has been Eq. (28), which is based on the suppression of the transverse photon momentum $|\mathbf{k}_\perp|$ with respect to the photon energy or longitudinal photon momentum by the Lorentz factor γ. As a matter of fact, one would expect the deviations of the equivalent photon cross section (32) from the "exact" cross section, where the external field approximation has also been applied, but no approximations about the transverse photon momentum $\mathbf{k}_\perp$ have been made, to be small; deviations should be of the same order $1/\gamma$ as the transverse components are suppressed over the longitudinal components. Numerical comparisons confirm this supposition.

If the integration over the impact parameter is not performed, expression (31) leads to an impact-parameter dependent differential cross section. The equivalent photon cross section (32) has been derived quite generally. The presented derivation does not depend on the explicit nature of the produced particle(s). An explicit derivation for the production of a scalar or pseudoscalar (spin 0) boson has been published previously [20].

E. Further illustration and interpretation

For a deeper insight expression (31) may be cast in a form being apparently closer to the equivalent photon method by folding the elementary cross section $\sigma_{\rm s}(\omega_1,\omega_2)$ and $\sigma_{\rm ps}(\omega_1,\omega_2)$ with the two-photon distribution functions $n_{\rm s}$ and $n_{\rm ps}$:

$$\frac{d^2\sigma}{db^2}(\mathbf{b}) = \int d\omega_1 \int d\omega_2 \left[n_{\rm s}(\omega_1,\omega_2;\mathbf{b})\sigma_{\rm s}(\omega_1,\omega_2) + n_{\rm ps}(\omega_1,\omega_2;\mathbf{b})\sigma_{\rm ps}(\omega_1,\omega_2) \right], \tag{33}$$

where

$$n_{\rm s/ps}(\omega_1,\omega_2;\mathbf{b}) = Z^4 e^4 \frac{\omega_1\omega_2}{\pi^2} \int \frac{d^2q_\perp}{(2\pi)^2}\, K^{(1)}_{ii'}(\mathbf{q}_\perp,\omega_1)\, K^{(2)}_{jj'}(-\mathbf{q}_\perp,\omega_2)\, \kappa^{ij}_{\rm s/ps}\kappa^{i'j'}_{\rm s/ps}\, e^{-i\mathbf{b}\cdot\mathbf{q}_\perp} \tag{34}$$

are the scalar and pseudoscalar two-photon distribution functions. The tensorial photon distribution function $K^{(n)}_{ii'}(\mathbf{q}_\perp,\omega)$ is defined by

$$K^{(n)}_{ii'}(\mathbf{q}_\perp,\omega) = \int \frac{d^2k_\perp}{(2\pi)^2}\, \mathcal{F}_n(\mathbf{k}_\perp,\omega)\, \mathcal{F}^*_n(\mathbf{k}_\perp - \mathbf{q}_\perp,\omega)\, \frac{k_i}{\omega}\, \frac{k_{i'} - q_{i'}}{\omega} \tag{35}$$

and describes the number of photons with definite mutual polarization to each other.

With the use of Fourier transforms for $K^{(n)}_{ii'}(\mathbf{q}_\perp,\omega)$ and the potential function $\mathcal{F}$ the two-photon distribution functions can be rewritten in terms of the transverse components of the electromagnetic fields themselves, which follows from the field strength tensor $F^{\mu\nu} = -i[k^\nu A^\mu(k_\sigma) - k^\mu A^\nu(k_\sigma)]$ using the electromagnetic potentials of Eq. (3); we arrive at

$$n_{\rm s}(\omega_1,\omega_2,\mathbf{b}) = \frac{1}{\pi^2\omega_1\omega_2} \int d^2x_\perp\, |\mathbf{E}_{1\perp}(\omega_1,\mathbf{x}_\perp - \mathbf{b}) \cdot \mathbf{E}_{2\perp}(\omega_2,\mathbf{x}_\perp)|^2 \tag{36}$$

and

$$n_{\rm ps}(\omega_1,\omega_2,\mathbf{b}) = \frac{1}{\pi^2\omega_1\omega_2} \int d^2x_\perp\, |\mathbf{E}_{1\perp}(\omega_1,\mathbf{x}_\perp - \mathbf{b}) \times \mathbf{E}_{2\perp}(\omega_2,\mathbf{x}_\perp)|^2 \quad . \tag{37}$$

We realize that not only the absolute magnitude but also the direction of the electromagnetic fields enter in the two-photon distributions. If the electromagnetic fields of the two nuclei are parallel to each other, they contribute to the scalar photon distribution function; if on the other side the electromagnetic fields are perpendicular to each other, they contribute to the pseudoscalar photon distribution.

With this in mind the illustration of the differential cross section (33) becomes straightforward: It consists of a scalar part, where the electromagnetic fields have to be parallel, and of a pseudoscalar part, where the electromagnetic fields have to be perpendicular.

For numerical purposes it is convenient to reduce the two-photon distributions to one-photon distribution functions. The one-photon distribution functions can be derived by equating the energy flux of the transverse electromagnetic fields of the moving nucleus, which is described by the Poynting vector, through an infinitesimal transverse plane element, which is characterized by its distance $\mathbf{b}$ to the trajectory of the nucleus, with the corresponding energy flux of a bunch of photons through the same plane element. It reads [21]

$$n(\omega;\mathbf{b}) = \frac{1}{\pi\omega} |\mathbf{E}_\perp(\mathbf{b},\omega)|^2 = \frac{4Z^2\alpha}{\omega} \left| \int \frac{d^2k_\perp}{(2\pi)^2}\, \mathbf{k}_\perp\, \frac{F(\mathbf{k}_\perp^2 + \omega^2/\gamma^2)}{\mathbf{k}_\perp^2 + \omega^2/\gamma^2}\, e^{-i\mathbf{b}\cdot\mathbf{k}_\perp} \right|^2 \tag{38}$$

and describes the number of photons with energy ω existing in a distance $|\mathbf{b}|$ from the center of the nucleus. $n(\omega,\mathbf{b})$ is of course independent of the direction of $\mathbf{b}$.

Then the two-photon distribution functions (36) and (37) can be expressed by two one-photon distribution functions. In the scalar case it results

$$n_{\rm s}(\omega_1,\omega_2;\mathbf{b}) = \int d^2x_\perp\, n(\omega_1;\mathbf{x}_\perp - \mathbf{b})\, n(\omega_2;\mathbf{x}_\perp) \times \left(\frac{(\mathbf{x}_\perp - \mathbf{b}) \cdot \mathbf{x}_\perp}{|\mathbf{x}_\perp - \mathbf{b}|\, |\mathbf{x}_\perp|} \right)^2 \tag{39}$$

and with a cross product in the pseudoscalar case,

$$n_{\rm ps}(\omega_1,\omega_2;\mathbf{b}) = \int d^2x_\perp\, n(\omega_1;\mathbf{x}_\perp - \mathbf{b})\, n(\omega_2;\mathbf{x}_\perp) \times \left(\frac{(\mathbf{x}_\perp - \mathbf{b}) \times \mathbf{x}_\perp}{|\mathbf{x}_\perp - \mathbf{b}|\, |\mathbf{x}_\perp|} \right)^2, \tag{40}$$

respectively. The two-photon distribution function essentially contains a product of one-photon distribution functions. The integration over $x_\perp$ means that the photon-photon interaction can take place over the whole perpendicular plane resulting in a product of local one-photon distribution functions. The expression in large brackets appears due to the dependence on the polarizations of the two photons.

The technical advantage of expressions (39) and (40) is the calculation of the two-photon distribution function by knowledge of the one-photon distribution function (38). In the case of a pointlike particle the function is known analytically [21]:

$$n(\omega;b) = \frac{Z^2\alpha}{\pi^2} \frac{\omega}{\gamma^2} \left[K_1\left(\frac{\omega b}{\gamma}\right) \right]^2, \tag{41}$$

which for large values of $\omega b/\gamma$ leads asymptotically to

$$n(\omega;b) \approx \frac{Z^2\alpha}{2\pi}\frac{1}{\gamma b}e^{-2\omega b/\gamma} \tag{42}$$

guaranteeing the convergence of the integral for large arguments b. For small b the photon distribution function $n(\omega;\mathbf{b})$ diverges because of the assumption of a pointlike particle. In the case of an extended particle the integral (38) has to be calculated numerically after performing a transformation to polar coordinates:

$$n(\omega;b) = \frac{Z^2\alpha}{\pi^2}\frac{1}{\omega}\left|\int_0^\infty dk_\perp\, k_\perp^2 \frac{F(k_\perp^2+\omega^2/\gamma^2)}{k_\perp^2+\omega^2/\gamma^2} J_1(bk_\perp)\right|^2 . \tag{43}$$

The convergence is guaranteed if the form factor vanishes fast enough to zero for $k_\perp \to \infty$. The form factors we use are the one for a homogeneously charged sphere

$$F_{\rm hcs}(-k^2) = \frac{3j_1(kR)}{kR}, \tag{44}$$

and the Gaussian form factor

$$F_{\rm G}(-k^2) = \exp\left(-\frac{k^2}{2Q_0^2}\right) . \tag{45}$$

In Fig. 1 we plot the impact-parameter dependent one-photon distribution function for a Pb nucleus at the maximum LHC energy ($\gamma = 3500$). Various form factors have been used. It is clear that the photon distribution of an extended nucleus with form factor has to agree with the one of a pointlike particle of the same charge Z for impact parameters larger than the nuclear radius ($R \approx 7$ fm). One can also see that the photon number scales with $1/\omega$ at low photon energies. On the other side the photon distribution breaks this scaling behavior for photon energies larger than $\omega = \gamma/b$ because of the large influence of the exponential function in (42).

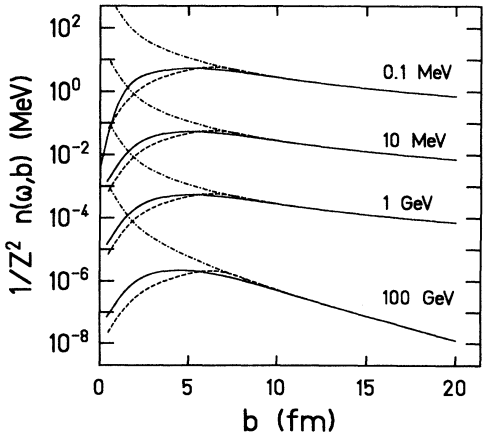

FIG. 1. One-photon distribution for a Pb nucleus and $\gamma = 3500$ as function of the impact parameter for different photon energies. The dash-dotted line corresponds to the form factor of a pointlike particle, the dashed line to the form factor of a homogeneously charged sphere with $R = 7.107$ fm and the solid line to a Gaussian form factor with $Q_0 = 60$ MeV.

The four-dimensional integrations in (33) with (39) and (40) were treated numerically with the adaptive Monte Carlo program VEGAS [22]. As a numerical test the integration over the impact parameter yields a very good agreement between the resulting total cross section and the corresponding equivalent photon cross section (1).

III. DISCUSSION OF THE RESULTS

In the first subsection we discuss generally the electromagnetic production of scalar and pseudoscalar bosons, whereas the second and third subsections are devoted to charged boson pairs and fermion pairs, respectively. We will concentrate on general aspects as, for example, the interplay between scalar and pseudoscalar contributions to the cross sections and reduction factors of the cross sections due to a nuclear overlap in the reaction. Here we will not depict any specific particle, exotic or not; this will be the exlusive subject of a subsequent publication [18], where we discuss the electromagnetic production and detectability of the Higgs bosons of the minimal supersymmetric extension of the standard model (MSSM) and various mesons, the supersymmetric partners of leptons and quarks and the supersymmetric partners of the $W^\pm$ boson and Higgs bosons, respectively. The electromagnetic production and detectability of the Higgs boson of the standard model has been discussed extensively in the literature before [4–17].

A. Electromagnetic production of scalar and pseudoscalar bosons

The scalar and pseudoscalar real two-photon fusion cross section $\sigma_{\rm s}$ and $\sigma_{\rm ps}$ enter in expression (33) for the differential cross section with respect to the impact parameter. Due to the vertex function (5) the pseudoscalar real two-photon fusion cross section $\sigma_{\rm ps}$ vanishes for the production of a scalar boson, i.e., $\sigma_{\rm ps}^{\gamma\gamma\to\text{s-boson}} = 0$; this means that the scalar boson can only be produced if the polarization vectors of the two photons are parallel to each other. For the production of a pseudoscalar boson it is the other way around; here the scalar real two-photon fusion cross section vanishes due to the vertex function (6), i.e., $\sigma_{\rm s}^{\gamma\gamma\to\text{ps-boson}} = 0$, so that the polarization of the two photons have to be orthogonal to each other. The two remaining polarized two-photon fusion cross sections, namely, $\sigma_{\rm s}^{\gamma\gamma\to\text{s-boson}}$ and $\sigma_{\rm ps}^{\gamma\gamma\to\text{ps-boson}}$, exhibit a similar structure:

$$\sigma_{\rm s(ps)}^{\gamma\gamma\to\text{s(ps)-boson}} = 2\frac{8\pi^2}{m_{\rm s(ps)\text{-boson}}}\Gamma_{\rm s(ps)\text{-boson}\to\gamma\gamma} \times\delta(s - m^2_{\rm s(ps)\text{-boson}}) . \tag{46}$$

This result can be easily derived from any standard QED textbook [19]; $m_{\rm s(ps)\text{-boson}}$ is the mass of the boson, $\Gamma_{\rm s(ps)\text{-boson}\to\gamma\gamma}$ denotes the two-photon decay width of the boson, and the Mandelstam variable s inside the bracket of the δ function is $s = 4\omega_1\omega_2$. The additional factor 2 in front of the right-hand side originates from definition (21).

Now we are able to study the dependence of the differential cross section (33) on the mass of the produced boson. It is convenient to use the normalized expression $\frac{1}{\sigma^{WW}}\frac{d\sigma}{db}$, where σ^{WW} is the total equivalent photon cross section (1) and $\frac{d\sigma}{db} = 2\pi b\, d^2\sigma/db^2$; here the factor $2\frac{8\pi^2}{m_b}\Gamma_{b\to\gamma\gamma}$ in (46) drops out and with that also the model dependence of the cross sections (46), which only enters in the two-photon decay width $\Gamma_{b\to\gamma\gamma}$. The only dependence of $\frac{1}{\sigma^{WW}}\frac{d\sigma}{db}$ on the boson mass stems from the remaining δ function, which gives rise to mass-dependent interferences in the integrations over the transverse momentum $\mathbf{q}_\perp$; confer again Eq. (33). Figures 2(a) and 2(b) show the results for the production of a scalar and pseudoscalar boson, respectively; masses of 100 MeV, 1 GeV, 10 GeV, and 100 GeV have been chosen. A Lorentz contraction factor of $\gamma = 3500$ (LHC) has been used for a Pb+Pb collision and the form factor (44) of a homogeneously charged sphere with radius $R = 7.1$ fm has been applied.

Let us focus on the scalar boson first; i.e., confer Fig. 2(a). With the increasing mass of the scalar boson, smaller impact parameters become more and more important. This is obvious because the heavier the boson becomes, the more it has to be produced in the vicinity of the strongest electromagnetic field densities of the two colliding heavy ions and that is near the nuclear surfaces, which corresponds to small impact parameters. In addition a double hump structure also shows up more pronounced as the mass of the scalar boson increases. This structure is smeared out for small masses; the reason for this is that the scalar boson has to be produced in a small volume, which should roughly be proportional to the cube of the Compton wavelength of the boson and therefore also be proportional to the inverse of the cube of the boson mass, so that for small boson masses this volume becomes relatively large and smears out any structure. The reason for the appearance of a double hump structure is related to the fact that the electromagnetic fields of the two colliding heavy ions have to be parallel in order to produce the scalar boson. The dip then should lie in the interval between once and twice the nuclear radius, so that the two nuclei overlap and the strong electromagnetic fields prevailing at their surfaces become to a major part perpendicular. Figure 2(a) shows the dip to lie at approximately $b = 9$ fm, which is larger than the nuclear radius $R = 7.1$ fm for Pb and smaller than $2R = 14.2$ fm.

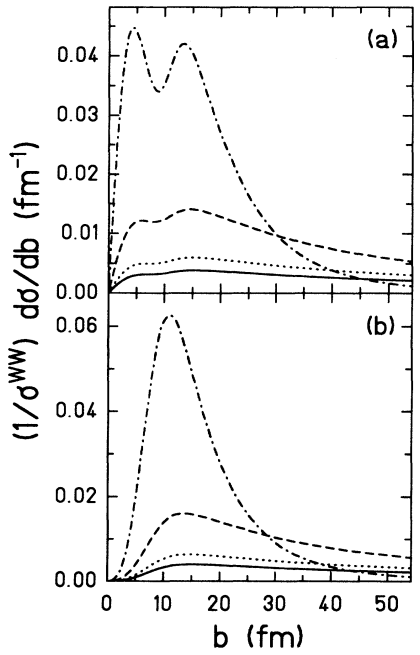

FIG. 2. Normalized impact-parameter dependent equivalent photon cross section for the production of (a) a scalar and (b) pseudoscalar boson. Four different scalar boson masses are considered: $m_b = 100$ MeV (solid line), 1 GeV (dotted line), 10 GeV (dashed line), and 100 GeV (dash-dotted line). A Lorentz contraction factor $\gamma = 3500$ (LHC) has been used for a Pb+Pb collision and the form factor (44) of a homogeneously charged sphere with radius $R = 7.1$ fm has been applied.

To support this suggestion further, i.e., that the dip is due to the orthogonality of the electromagnetic fields, we now turn our attention to the production of a pseudoscalar boson. For such a particle the electromagnetic fields have to be perpendicular. As a consequence, the maximum of the corresponding impact-parameter dependent cross section should approximately be at impact parameters, which correspond to the dip before.

The structure of the impact-parameter dependent cross section for the production of a pseudoscalar boson is not affected by the boson mass, so that always only one maximum occurs; this is demonstrated in Fig. 2(b). The double hump structure in case of a heavy scalar boson smears out, if instead of a form factor of a homogeneously charged sphere one of a Gaussian charge distribution is used. Because the nuclear surface is smeared out in the Gaussian case, the dip is no longer enhanced [20].

For a good experimental detectability of the electromagnetically produced particles two presuppositions have to be fullfilled: relatively clean signals from the decay channels of the produced particles and a trigger on peripheral collisions of the heavy ions. Whereas the first part will be the subject of a subsequent publication [18], we now would like to concentrate on the second point.

Small impact parameters have to be excluded in order to discard central collisions and the accompanying large hadronic background for the particle detection; this motivates the introduction of a sharp cutoff impact parameter $b_C = 2R$, which leads to a reduced total cross section

$$\sigma^{\rm red}_{A_1A_2\to A_1A_2b} = \int_0^\infty db \frac{d\sigma_{A_1A_2\to A_1A_2b}}{db}\,\Theta(b-2R), \tag{47}$$

R denotes the nuclear radius. In Figs. 3(a) and 3(b) we display this reduction factor $\sigma^{\rm red}_{A_1A_2\to A_1A_2b}/\sigma^{WW}_{A_1A_2\to A_1A_2b}$ in dependence on the scalar and pseudoscalar boson mass for LHC ($\gamma = 3500$, lower curve) and SSC ($\gamma = 8000$, upper curve) energies.

For small boson masses, i.e., $m_b < 1$ GeV, the reduced cross section $\sigma^{\rm red}$ is practically identical to the total cross

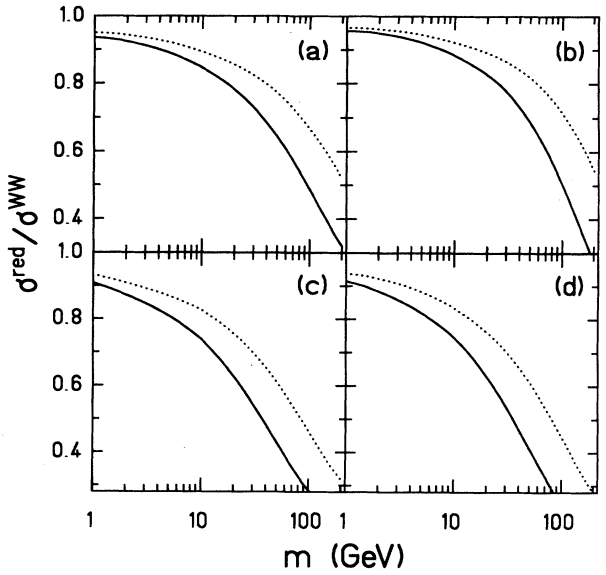

FIG. 3. Reduction factors σ^{red}/σ^{WW} in dependence on (a) the scalar boson, (b) pseudoscalar boson, (c) charged boson, and (d) fermion mass for LHC ($\gamma = 3500$, solid line) and SSC ($\gamma = 8000$, dotted line) energies.

section; this statement holds true for both the scalar and the pseudoscalar boson. This becomes clear in view of Figs. 2(a) and 2(b); note that the area under each curve of Figs. 2(a) and 2(b) is unity. For small boson masses the dominant contribution to the total cross section results from large impact parameters and the contribution from small impact parameters is negligible. For light neutral bosons, such as, for example, the mesons, it has the consequence that already the total equivalent photon cross section σ^{WW} describes their electromagnetic production and that σ^{WW} is relevant for the experiments. For bosons with a higher mass, the contribution from small impact parameters becomes more and more important. Their contribution will be cut off in the reduced cross section (47); for an increasing boson mass the reduction factor σ^{red}/σ^{WW} will deviate from 1 and decrease more and more. For a scalar boson mass $m_b = 50$ GeV the reduction factor is $\sigma^{red}/\sigma^{WW} = 0.6$ (LHC) and 0.8 (SSC) and for $m_b = 200$ GeV we found $\sigma^{red}/\sigma^{WW} = 0.3$ (LHC) and 0.5 (SSC). For a pseudoscalar boson the reduction factors are very similiar; for $m_b = 50$ GeV we obtained $\sigma^{red}/\sigma^{WW} = 0.7$ (LHC) and 0.8 (SSC) and for $m_b = 200$ GeV we computed $\sigma^{red}/\sigma^{WW} = 0.3$ (LHC) and 0.5 (SSC).

Observe that the reduction factors do not depend on the specific nature of the scalar and the pseudoscalar boson. They only depend on the mass of the scalar or pseudoscalar boson and on the Lorentz contraction factor γ, which reflects the collision energy of the heavy ions. Contrary to the reduction factor σ^{red}/σ^{WW} a model dependence for the scalar or pseudoscalar boson enters for the absolute reduced cross section (47). The crucial quantity is the two-photon decay width entering in the elementary scalar or pseudoscalar two-photon fusion cross section (46); it strongly depends on the specific nature of the particle.

B. Electromagnetic production of a charged boson pair

For the scalar or pseudoscalar boson either the polarized pseudoscalar or scalar elementary two-photon fusion cross section vanishes. For the electromagnetic production of a charged boson pair both polarized two-photon fusion cross sections contribute; they are given in lowest order in α by

$$\sigma_s^{\gamma\gamma\to b^+b^-} = \frac{2\pi\alpha^2}{s}\left[\sqrt{1-\frac{4m_b^2}{s}}\left(1+\frac{6m_b^2}{s}\right) - \frac{4m_b^2}{s}\left(2-\frac{6m_b^2}{s}\right)\ln\left(\frac{\sqrt{s}}{2m_b}+\sqrt{\frac{s}{4m_b^2}-1}\right)\right]\Theta(s-4m_b^2) \tag{48}$$

and

$$\sigma_{ps}^{\gamma\gamma\to b^+b^-} = \frac{2\pi\alpha^2}{s}\left[\sqrt{1-\frac{4m_b^2}{s}}\left(1+\frac{2m_b^2}{s}\right) - \frac{4m_b^2}{s}\left(2-\frac{2m_b^2}{s}\right)\ln\left(\frac{\sqrt{s}}{2m_b}+\sqrt{\frac{s}{4m_b^2}-1}\right)\right]\Theta(s-4m_b^2) \quad . \tag{49}$$

m_b represents the mass of one charged boson.

Again it is most convenient to consider the normalized expression $\frac{1}{\sigma^{WW}}\frac{d\sigma}{db}$; its mass dependence can be traced back to the polarized cross sections Eqs. (48) and (49) in combination with the interferences arising from the integration over $\mathbf{q}_\perp$ in (34). Figure 4 depicts the normalized differential cross section for four different boson masses, namely $m_b = 100$ MeV, 1 GeV, 10 GeV, and 100 GeV, for a Pb + Pb collision at the maximum LHC energy ($\gamma = 3500$). Observe that the area under each curve (solid line) of the normalized differential cross section is unity, although some of them have been rescaled with an indicated factor. The differential cross section consists of a scalar contribution (dotted), where the electromagnetic fields of the two colliding heavy ions have to be parallel to produce the charged boson pair, and a pseudoscalar contribution (dashed), where the electromagnetic fields have to be perpendicular. As expected from our discussions in the previous section a double hump structure shows up for the scalar part and the maximum of the pseudoscalar part falls into the dip of the scalar differential cross section. At the highest considered boson mass the scalar contribution dominates tremendously over the pseudoscalar contribution. This traces back to the dominance of the polarized scalar elementary two-photon cross section (48) over the pseudoscalar one (49) near threshold production. Exactly at threshold ($s = 4m_b^2$) the charged boson pair is created with no kinetic energy in

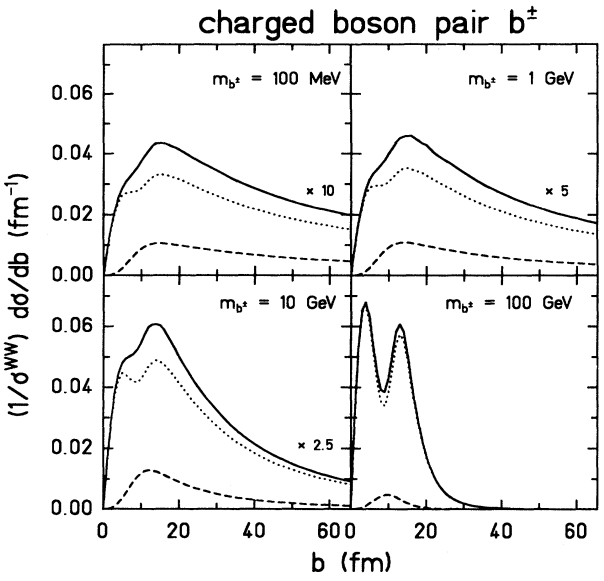

FIG. 4. Impact-parameter dependent differential cross section for the electromagnetic production of a charged boson pair (solid line) with scalar (dotted line) and pseudoscalar (dashed line) contribution and normalized to the total cross section σ^{WW}. The results for the boson masses m_b = 100 MeV, 1 GeV, and 10 GeV have been multiplied with factors of 10, 5, and 2.5, respectively. A Pb + Pb collision at the maximum LHC energy (γ = 3500) with the form factor (44) has been considered.

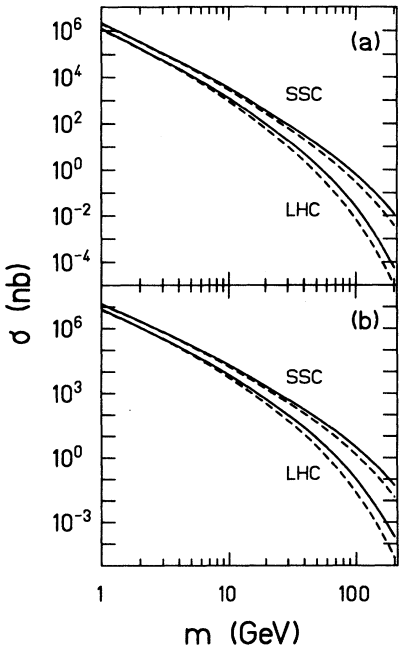

FIG. 5. Total (solid line) and reduced (dashed line) cross sections for the production of (a) a charged boson and (b) fermion pair in a Pb + Pb collision in dependence on the mass of the charged boson and fermion, respectively.

the c.m. system of the two photons and therefore can be understood as a composite scalar boson consisting of either two scalar charged bosons or two pseudoscalar charged bosons; for the electromagnetic production of a neutral scalar boson the electromagnetic fields have to be parallel, so that only a scalar contribution to the cross section should be important. The dominance of the scalar polarized two-photon fusion cross section over the pseudoscalar one also leads to a double-hump-like, i.e., scalarlike, appearance of the impact-parameter dependent differential cross section $d\sigma/db$ for large boson masses. At lower boson masses the double hump structure of the scalar cross section is smeared out, because of the increasing production volume of the charged boson pair, which should roughly be proportional to the inverse cube of the boson mass; confer also the discussions in the last section. Also the pseudoscalar cross section becomes more and more important, so that in addition its maximum, which falls into the dip of the scalar cross section, again smears out the double hump structure of the scalar part. As a consequence, the dip disappears completely for the impact-parameter dependent differential cross section $d\sigma/db$ at small boson masses.

If the central impact parameter regime, i.e., $b \leq 2R$, where R is the nuclear radius of the heavy ion, is cut off according to Eq. (47), then the reduction factor $\sigma^{\rm red}/\sigma^{WW}$ should be approximately 1 for small boson masses, because only a minor part in the differential cross section is cut off. But for large boson masses a major part is cut off with the small impact parameters, so that the reduction factors should deviate significantly from 1. This situation is verified in Fig. 3(c). For a mass of the charged boson of $m_{b^{\pm}}$ = 50 GeV the reduction factor is $\sigma^{\rm red}/\sigma^{WW} = 0.4$ for LHC and $\sigma^{\rm red}/\sigma^{WW} = 0.6$ for SSC; for $m_{b^{\pm}}$ = 200 GeV it follows $\sigma^{\rm red}/\sigma^{WW} = 0.2$ (LHC) and $\sigma^{\rm red}/\sigma^{WW} = 0.3$ (SSC).

The reduction factors only depend on the mass of the charged boson and on the Lorentz contraction factor γ. Figure 5(a) shows the absolute total cross section σ^{WW} and the absolute reduced total cross section $\sigma^{\rm red}_{\rm PbPb\to PbPb+b^+b^-}$ for the production of a charged boson pair in lowest order in the fine structure constant α.

For a charged boson mass of 50 GeV and 100 GeV the reduced electromagnetic production cross section is about 1 nb and 0.01 nb, respectively, for a Pb + Pb collision at LHC energies (γ = 3500). For an expected LHC luminosity of 10^{28} cm^{-2} sec^{-1} and a running time of 10^7 sec/yr ($\approx \frac{1}{3}$ yr) about 100 charged bosons with mass $m_{b^{\pm}}$ = 50 GeV and about 1 charged boson with mass $m_{b^{\pm}}$ = 100 GeV could be produced electromagnetically in a Pb + Pb collision.

C. Electromagnetic production of a fermion pair

For the electromagnetic production of a fermion pair both the polarized scalar and pseudoscalar two-photon fusion cross sections contribute. They read in lowest order in α [23]

$$\sigma_{\rm s}^{\gamma\gamma\to f^+f^-} = \frac{4\pi\alpha^2}{s}\left[\left(1+\frac{4m_f^2}{s}-\frac{12m_f^4}{s^2}\right)2\ln\left(\frac{\sqrt{s}}{2m_f}+\sqrt{\frac{s}{4m_f^2}-1}\right)-\left(1+\frac{6m_f^2}{s}\right)\sqrt{1-\frac{4m_f^2}{s}}\right]\Theta(s-4m_f^2) \quad (50)$$

and

$$\sigma_{\rm ps}^{\gamma\gamma\to f^+f^-} = \frac{4\pi\alpha^2}{s}\left[\left(1+\frac{4m_f^2}{s}-\frac{4m_f^4}{s^2}\right)2\ln\left(\frac{\sqrt{s}}{2m_f}+\sqrt{\frac{s}{4m_f^2}-1}\right)-\left(1+\frac{2m_f^2}{s}\right)\sqrt{1-\frac{4m_f^2}{s}}\right]\Theta(s-4m_f^2) \quad . \quad (51)$$

Figure 6 depicts the normalized differential cross section for four different fermion masses, namely, m_f = 100 MeV, 1 GeV, 10 GeV, and 100 GeV, for a Pb + Pb collision at the maximum LHC energy (γ = 3500). The differential cross section consists of a scalar (dotted) and a pseudoscalar contribution (dashed). The maximum of the pseudoscalar part falls into the dip of the double hump structure of the scalar differential cross section, as expected. With increasing fermion mass the pseudoscalar contribution dominates more and more over the scalar contribution, which is contrary to the production of a charged boson pair. This traces back to the dominance of the polarized pseudoscalar elementary two-photon cross section (51) over the scalar one (50) near threshold production. Exactly at threshold ($s = 4m_f^2$) the fermion pair is created with no kinetic energy in the c.m. system of the two photons and therefore can be understood as a composite boson with spin 0; a spin-1 boson cannot be created by two photons [24]. This composite spin-0 boson resembles a fermionium, which has negative parity in its ground state [24]. Therefore it is a pseudoscalar composite boson consisting of a fermion pair. The dominance of the pseudoscalar polarized two-photon fusion cross section over the scalar one leads to a pseudoscalar-like appearance, i.e., only one maximum, of the impact-parameter dependent differential cross section $d\sigma/db$ for large fermion masses. For lower fermion masses the situation is similiar; the scalar contribution increases, but also the double hump structure smears out, so that again $d\sigma/db$ is a simple curve with one maximum.

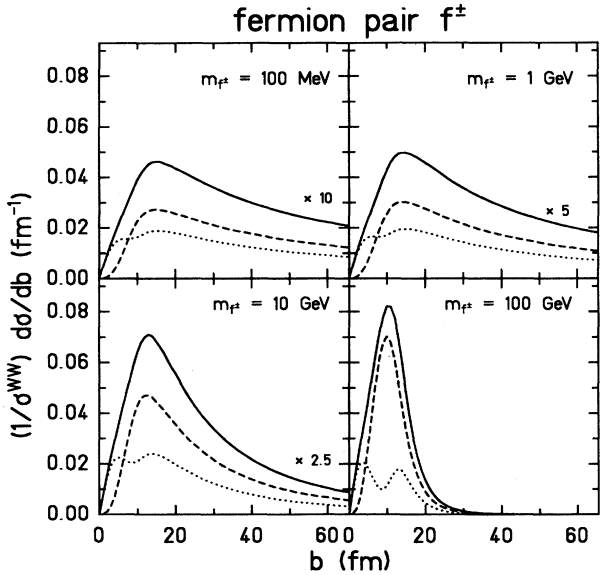

FIG. 6. Impact-parameter dependent differential cross section (solid line) for the electromagnetic production of a fermion pair with scalar (dotted line) and pseudoscalar (dashed line) contribution and normalized to the total cross section σ^{WW}. The results for the fermion masses m_f = 100 MeV, 1 GeV, and 10 GeV have been multiplied with factors of 10, 5 and 2.5, respectively. A Pb + Pb collision at the maximum LHC energy (γ = 3500) with the form factor (44) has been considered.

If the central impact-parameter regime, i.e., $b \le 2R$, is cut off according to Eq. (47), then the reduction factor $\sigma^{\rm red}/\sigma^{WW}$ should be approximately 1 for small fermion masses, because only a very small part in the differential cross section is cut off. But for large fermion masses a major part is cut off with the small impact parameters, so that the reduction factors should decrease significantly from 1. This situation is exemplified in Fig. 3(d). For a mass of the fermion of m_f = 50 GeV the reduction factor is $\sigma^{\rm red}/\sigma^{WW} = 0.4$ for LHC and $\sigma^{\rm red}/\sigma^{WW} = 0.6$ for SSC; for m_f = 200 GeV we obtained $\sigma^{\rm red}/\sigma^{WW} = 0.1$ (LHC) and $\sigma^{\rm red}/\sigma^{WW} = 0.3$ (SSC).

Figure 5(b) shows the absolute total cross section σ^{WW} and the absolute reduced total cross section $\sigma^{\rm red}_{\rm PbPb\to PbPb+f^+f^-}$ for the production of a fermion pair in lowest order in the fine structure constant α. For very light fermions, such as leptons $(e^\pm, \mu^\pm, \tau^\pm)$ and quarks (u, d, s, c) in the 1 MeV to 1 GeV mass regime, the electromagnetic production cross sections are very high; but here higher-order corrections in α have to be taken into account. For fermion pairs with a much higher mass, higher-order effects should be again of minor importance. For a fermion mass of 50 GeV and 100 GeV the reduced electromagnetic production cross section is about 4 nb and 0.03 nb, respectively, for a Pb + Pb collision at LHC energies (γ = 3500). This corresponds to 400 and 3, respectively, electromagnetically produced fermion pairs with mass m_f = 50 GeV and 100 GeV, respectively, per yr in a Pb + Pb collision.

IV. CONCLUSIONS

We presented a general derivation of the equivalent photon method from QED, which treats the electromagnetic production of scalar and pseudoscalar (spin 0) bosons, charged (spin 0) boson, fermion pairs, charged (spin 1) bosons, etc., on the same footing. The external field approximation has been employed, which assumes the two colliding heavy ions move on straight trajectories

with constant velocity and are characterized by their classical electromagnetic fields. The crucial approximation results from the observation that the transverse momentum components of the virtual photons are suppressed by the Lorentz contraction factor γ over their longitudinal components and their energy. Deviations of the equivalent photon cross sections from exact cross sections are of order $1/\gamma$; for LHC (SSC) energies we have $\gamma = 3500$ (8000).

As a by-product an expression for the impact-parameter dependent differential cross section could also be derived; it maintains some of the simplicity of the equivalent photon approach and its integration over the impact parameter yields the total equivalent photon cross section. As the impact-parameter dependence is concerned, it is not the elementary two-photon fusion cross section averaged over the photon polarizations which enters in the equivalent photon cross section, but rather the two polarized elementary two-photon fusion cross sections. For the scalar polarized cross section the polarization vectors of the two photons are parallel, whereas for the pseudoscalar cross section they are perpendicular. This has as consequences for the impact-parameter dependent differential cross section that for the scalar contribution the electromagnetic fields of the two colliding heavy ions have to be parallel and that for the pseudoscalar contribution have to be perpendicular.

For the electromagnetic production of a scalar (spin 0) boson only the scalar polarized two-photon fusion cross section contributes to the impact-parameter dependent cross section. For a pseudoscalar (spin 0) boson it is the other way around, only the pseudoscalar polarized two-photon fusion cross section contributes. For the electromagnetic production of a charged (spin 0) boson pair and a fermion pair the scalar as well as the pseudoscalar polarized two-photon fusion cross sections contribute. In the limit of very large masses of charged bosons it is the scalar part which dominates over the pseudoscalar part, so that the electromagnetic fields have to be parallel. If the fermion mass becomes very large it is then the pseudoscalar part which dominates over the scalar part, so that the electromagnetic fields are mainly perpendicular.

In order to provide a clean experimental trigger on the two heavy ions or its fission products, the central impact parameter regime has to be excluded. A simple cutoff of this regime leads to reduction factors of the total equivalent photon cross section depending on the mass and nature (i.e., scalar or pseudoscalar boson, charged boson pair, fermion pair) of the produced particle or particles and on the beam energy. This reduction factor remains about 1 up to masses of approximately 1 GeV and can decrease to approximately 1/10 for masses of about 200 GeV. This decrease for heavy masses is not crucial; with an expected LHC luminosity of 10^{28} cm^{-2} sec^{-1} and a running time of 1/3 yr still about 100 (1) charged boson pairs with mass $m_{b^\pm} = 50$ GeV (100 GeV) and about 400 (3) fermion pairs with mass $m_{f^\pm} = 50$ GeV (100 GeV) can be produced. In conclusion, at LHC energies exotic particles with masses up to 200 GeV could be produced electromagnetically in ultrarelativistic heavy-ion collisions.

One of us (M.G.) wants to thank the Alexander von Humboldt Stiftung for its support with the Feodor Lynen Foundation.

[1] E. Fermi, Z. Phys. **29**, 315 (1924).
[2] E. J. Williams, Proc. R. Soc. London A **139**, 163 (1933).
[3] C. Weizsäcker, Z. Phys. **88**, 612 (1934).
[4] M. Grabiak, B. Müller, W. Greiner, G. Soff, and P. Koch, J. Phys. G **15**, L25 (1989).
[5] G. Soff, J. Rau, M. Grabiak, B. Müller, and W. Greiner, in *The Nuclear Equation of State*, edited by W. Greiner and H. Stöcker (Plenum, New York, 1989), Part B, p. 579.
[6] M. Drees, J. Ellis, and D. Zeppenfeld, Phys. Lett. B **223**, 454 (1989).
[7] R. N. Cahn and J. D. Jackson, Phys. Rev. D **42**, 3690 (1990).
[8] E. Papageorgiu, Phys. Lett. B **250**, 155 (1990).
[9] G. Baur and L.G. Ferreira Filho, Nucl. Phys. **A518**, 786 (1990).
[10] J. S. Wu, C. Bottcher, M. R. Strayer, and A. K. Kerman, Ann. Phys. (N.Y.) **210**, 402 (1991).
[11] B. Müller and A. J. Schramm, Phys. Rev. D **42**, 3699 (1990).
[12] K. J. Abraham, R. Laterveer, J. A. M. Vermaseren, and D. Zeppenfeld, Phys. Lett. B **251**, 186 (1990).
[13] J. W. Norbury, Phys. Rev. D **42**, 3696 (1990).
[14] Ch. Hofmann, G. Soff, A. Schäfer, and W. Greiner, Phys. Lett. B **262**, 210 (1991).
[15] J. Eichler, Phys. Rep. **193**, 165 (1990).
[16] C. A. Bertulani and G. Baur, Phys. Rep. **161**, 299 (1988).
[17] K. J. Abraham, M. Drees, R. Laterveer, E. Papageorgiu, A. Schäfer, G. Soff, J. Vermaseren, and D. Zeppenfeld, in Proceedings of the Coherent Processes in Heavy Ion Collisions at the LHC, Large Hadron Collider Workshop, Aachen, 1990, edited by G. Jarlskog and D. Rein (CERN Report No. 90-10, ECFA 90-133, 1990), Vol. II, p. 1224.
[18] M. Greiner, M. Vidović, and G. Soff, Phys. Rev. C **47**, 2288 (1993), this issue.
[19] J. D. Bjorken and S. D. Drell, *Relativistic Quantum Mechanics* (McGraw–Hill, New York, 1964).
[20] M. Greiner, M. Vidović, J. Rau, and G. Soff, J. Phys. G **17**, L45 (1991).
[21] J. D. Jackson, *Classical Electrodynamics* (Wiley, New York, 1975).
[22] G. P. Lepage, J. Comput. Phys. **27**, 192 (1978).
[23] V. M. Budnev, I. F. Ginzburg, G. V. Meledin, and V. G. Serbo, Phys. Rep. **15**, 181 (1975).
[24] T. D. Lee, *Particle Physics and Introduction to Field Theory* (Harwood Academic, Chur, 1981).